Surface Plasmon Polaritons

DOI: 10.1002/anie.200904646

Periodic Electric Field Enhancement Along Gold Rods with Nanogaps**

María L. Pedano, Shuzhou Li, George C. Schatz, and Chad A. Mirkin**

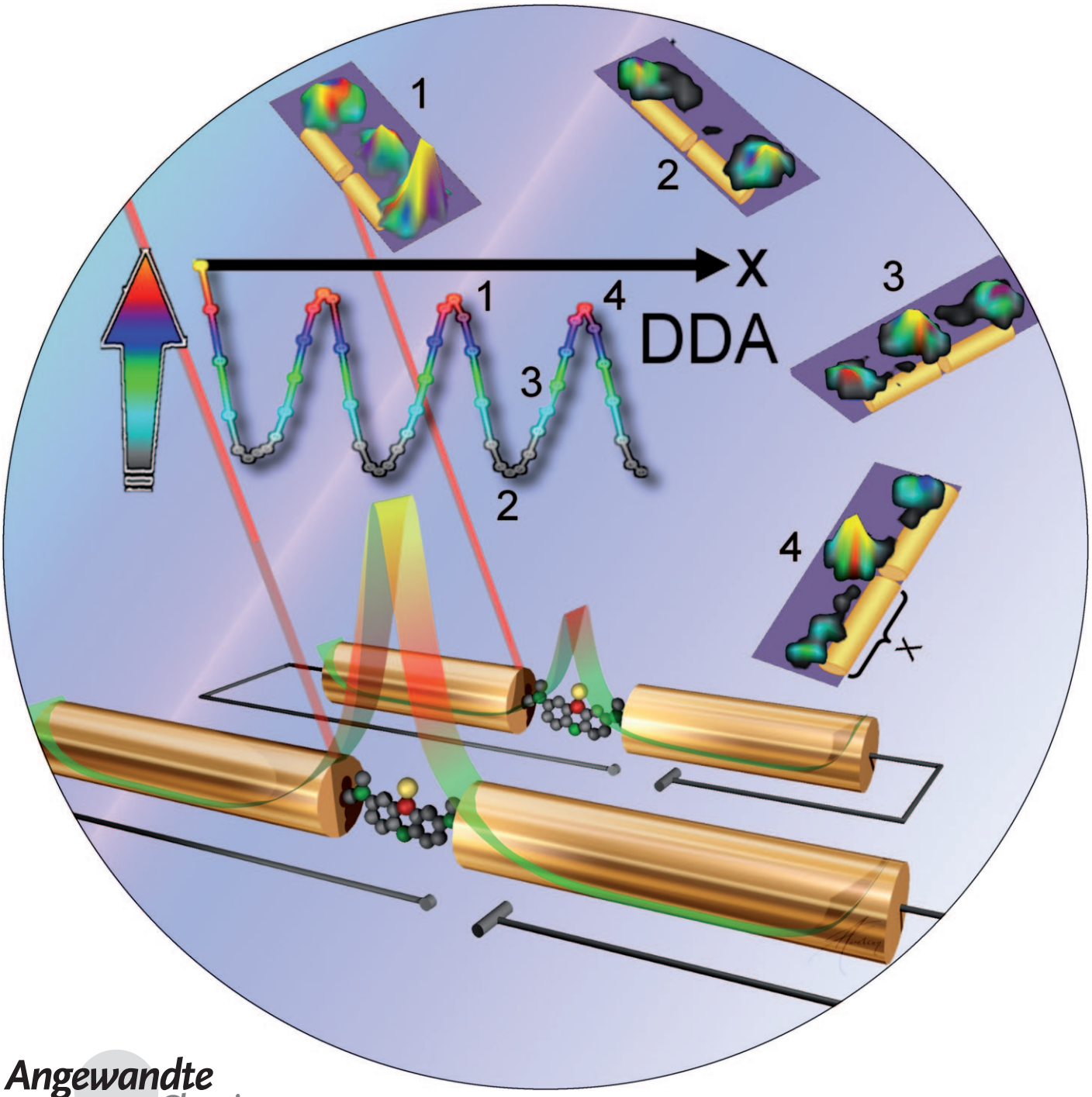

Over the past five years, we have been developing a novel electrochemistry-enabled nanofabrication technique known as on-wire lithography (OWL).[1] This technique allows control of the chemical composition and architecture of a one-dimensional wire from the nanometer to micrometer length scale.[1,2] Periodic structures that consist of gaps as small as 2 nm and segment lengths that span the 20 nm to many micrometer length scale have been synthesized by OWL.[3] These structures have been used to create a wide variety of functional architectures, including molecular transport junctions,[3] electrical nanotraps,[4] catalysts,[5] chemically driven nanomachinery,[5] bioseparation materials,[6,7] and probes for biodiagnostics assays.[8] OWL is particularly useful for creating plasmonically active structures from noble metals such as Au and Ag.[2,9] Recently, we demonstrated that by tailoring disk (120 nm thick, 360 nm diameter) and gap sizes (30 nm) in one-dimensional Au nanostructures, one could create Raman hotspots,[10] which have been optimized for spectroscopic identification purposes.[8] However, from the calculations carried out in the same work, it was implied and later observed (Figure 1) that the signal enhancement within the gap of these structures dramatically decays with increasing rod segment length. For example, no significant Raman signal is obtained for a 10 nm gap within 3 μm long segments, while significant, measurable signals arise from disk pairs made of shorter segments (120 nm) attached as an internal reference (Figure 1 B). This behavior poses the challenge of creating nanogap structures with large signal enhancements and long segment lengths. These structures can be used as addressable electrodes where electrical transport measurements can be coupled with the ability to spectroscopically characterize the gap composition by surface-enhanced Raman scattering (SERS).[11,12] The optical properties of single nanorods[13–19] and certain dimers[20,21] have recently been studied. However, no simultaneous theoretical and experimental study has been reported on the effect of the geometrical parameters of gapped nanorods on the electromagnetic enhancement factor (EF) at the gap. Herein, we attempt to elucidate the structural factors that lead to maximized signal enhancement in nanogap structures

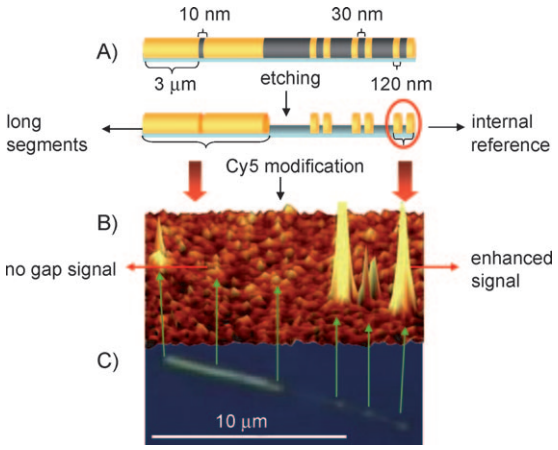

Figure 1. A) Schematic representation of a nanostructure generated by OWL, before and after sacrificial Ni etching. The nanostructure bears a long segment (3 μm) Au nanorod with 10 nm gap spacing, and three Au disk pairs with an optimized geometry (120 nm Au disk and 30 nm gap) to obtain Raman hot spots.[10] The nanostructures were modified with 23-mer oligonucleotides bearing a Cy5 Raman dye; B) Raman scan showing the integrated signal from the Cy5 dye at 1447 cm^{-1}; C) the optical microscope image of the nanostructure in (B).

as a function of electrode segment length. Significantly, we have determined that the SERS enhancement and localized fields in the gap simply do not monotonically decrease with segment length but rather are a periodic function of segment length; therefore, one can indeed create idealized geometries that have both macroscopically addressable long segments and nanogaps that lead to a high signal enhancement.

As a first attempt to identify an optimum geometry of gapped Au nanorods with signal-enhancing capabilities, we performed discrete dipole approximation (DDA) calculations for the EF contribution at the gap as a function of segment length (Figure 2). The incident wavelength, gap length, and the rod diameter were fixed at 633, 24, and 360 nm, respectively. The incident polarization is taken to be parallel to the rod axis, and the wave vector is perpendicular to the axis. The EF equals $|E|^4/|E_0|^4$, where E and E_0 are the local and incident electric fields, respectively, averaged over the surfaces of the rod at the gap. The curve represents the EF variation versus segment length for a symmetric gapped rod, where the two segments are exactly the same. The segment lengths are equally varied for both sides from 40 to 2000 nm in

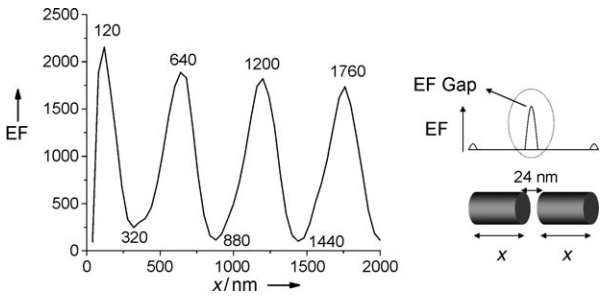

Figure 2. DDA simulation of the EF obtained at a 24 nm gap when varying symmetrically both segment lengths *x*.

[*] Dr. M. L. Pedano,[+] Dr. S. Li,[+] Prof. G. C. Schatz, Prof. C. A. Mirkin
Department of Chemistry and
International Institute for Nanotechnology, Northwestern University
2145 Sheridan Road, Evanston, IL 60208 (USA)
Fax: (+1) 847-467-7302
E-mail: schatz@chem.northwestern.edu
chadnano@northwestern.edu
Homepage: http://chemgroups.northwestern.edu/mirkingroup
[+] These authors contributed equally to this work.
[**] SEM work was performed in the (EPIC) (NIFTI) (Keck-II) facility of NUANCE Center at Northwestern University. The NUANCE Center is supported by NSF-NSEC, NSF-MRSEC, the Keck Foundation, the State of Illinois, and Northwestern University. C.A.M. acknowledges support from a NSSEF Fellowship from the DoD. C.A.M. and G.C.S. acknowledge the National Science Foundation (NSF) for support of this research. M.L.P. acknowledges the Schlumberger Foundation for Fellowship support through a FFTF Award.
Supporting information for this article is available on the WWW under http://dx.doi.org/10.1002/anie.200904646.

increments of 40 nm. The EF intensity oscillates periodically with the segment length every 560 nm without significant decay. The period of the EF oscillations for segments on gapped rods (560 nm) is a little smaller than the period of surface plasmon polaritons (SPPs; 600 nm, Figure S1 in the Supporting Information) that propagate along a single infinite 360 nm diameter Au rod when the wavelength of the incident light is 633 nm.[22] Maxima occur at 120, 640, 1200, and 1760 nm. The 120 nm rod length associated with the lowest order mode is roughly one-quarter of the SPP wavelength λ_{SPP}, which is consistent with previous observations.[10] This length arises from a 45° phase pickup in the boundary conditions, which are satisfied by SPPs that reflect at the ends of the rods.[16] All the maxima correspond to excitation of the odd-order plasmon multipole modes of each segment.[17] Excitation of even-order modes is symmetry-forbidden for isolated rods with this choice of polarization and wavevector.[15,17] Figure 2 shows that at least for a 24 nm gap, the SPP period correctly explains the calculated periodicity in the EF. We now show that the same periodicity is observed experimentally (Figure 3).

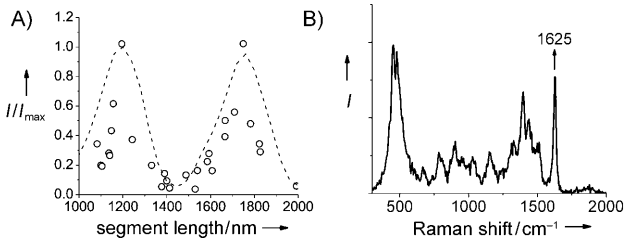

Figure 3. A) Normalized SERS intensities measured at a 24 nm gap as a function of the rod segment length *x* (both rod segments are fixed at the same length for each data point). The curves show experimental results (○) for the total integrated signal at 1625 cm^{-1} MB spectral band, where it scatters strongly, and a comparison (-----) with theoretical calculations shown in Figure 2. B) A MB SERS spectrum on a gapped Au rod.

We employed the OWL procedure to produce gapped nanorods of different segment lengths. Briefly, for each defined segment length, Au nanorods were electrodeposited inside Ag-evaporated anodic aluminum oxide (AAO) templates by applying the desired charge through the corresponding electroplating solution (Technic, Inc.) in a three-electrode electrochemical cell.[1] To grow the first segment (S_1), it was necessary to apply a continuous charge (Q_1) according to a previously determined calibration curve. Then, a Ni layer was deposited as a sacrificial layer to form the gap after Ni etching. The second Au segment was deposited from a normal plating solution by applying a continuous charge (Q_2) following a conventional calibration curve.[1] By following this procedure, we synthesized different batches of rods with several dimensions that were characterized by SEM (Figure S2 in the Supporting Information). The average measured distances for segment lengths and gap sizes were as follows: batch 1) $S_1 = (1274 \pm 87)$ nm, gap $= (25 \pm 7)$ nm, $S_2 = (1194 \pm 98)$ nm; batch 2) $S_1 = (1584 \pm 76)$ nm, gap $= (20 \pm 10)$ nm, $S_2 = (1555 \pm 114)$ nm; batch 3) $S_1 = (1719 \pm 77)$ nm, gap $= (17 \pm 11)$ nm, $S_2 = (1809 \pm 135)$ nm. After the OWL process, the gapped Au rods were modified with an ethanolic solution of methylene blue (MB; 1 mM), washed, and characterized by scanning SERS.

Figure 3A shows the normalized SERS intensity obtained at the gaps of the rods; each point is based upon integration of the MB band between 1590 and 1660 cm^{-1} (Figure 3B) and plotted as a function of the Au segment length. Normalized theoretical results from Figure 2 are presented in Figure 3A for comparison. Peak intensities from both experimental and theoretical results have been separately normalized to unity. Sample SERS scans and the corresponding SEM images of the scanned rods are shown in Figure 4A and B, respectively; rods with segment lengths corresponding to the two maxima and middle minimum of the curve in Figure 3A were chosen as representative examples.

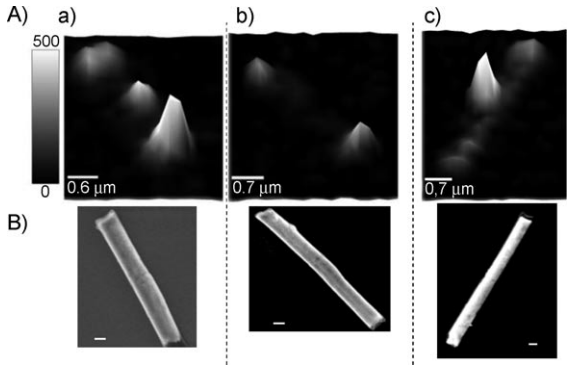

Figure 4. A) SERS scans integrating the 1625 cm^{-1} MB spectral band (scale bar: CCD counts) and B) the corresponding SEM images of the rods. The images in (A) and (B) represent rod segment lengths corresponding to a) the first maximum (*x*: 1200 nm; *y*: 520), b) middle minimum (*x*: 1400 nm; *y*: 46), and c) second maximum gap intensity (*x*: 1750 nm; *y*: 510) of the curve shown in Figure 3A. Scale bar in (B): 200 nm. *x* = segment length, *y* = absolute experimental Raman intensity.

The experimental results are in good agreement with the theoretical results (Figure 3A), and demonstrate a 560 nm EF periodicity and relative maximum and minimum peak intensities obtained at the predicted segment lengths. The difference in theoretical and experimental intensities can be attributed in part to imperfections in the gapped nanorod structures. Indeed, there is experimental variability in gap distance, the symmetry and segment length, and gap roughness of the synthesized rods within individual rods, and from rod to rod. Since the AAO templates that were used to grow the rods have a 10% uncertainty in pore size distribution, there are variations in segment lengths and gap sizes, even within the same batch, and even when rods are deposited under the same plating conditions. We and other research groups have shown that SERS signals depend on gap distance,[10,16] surface roughness,[23] and also on the segment length, as shown in Figure 2 and Figure 3. However, as we discuss in the following sections, although these variations cause fluctuations in the EF dependence on segment length

(Figure 3A), they do not significantly affect the observed 560 nm periodicity.

To account for the effect of gap variations and gap roughness on the SERS intensities, the dependence of the EF on the gap distance was studied using DDA calculations for a simulated smooth and rough gap (Figure 5A and B, respectively). The segment length was fixed at 1200 nm in both

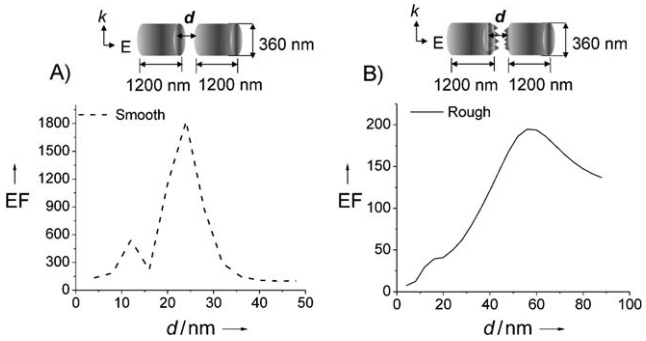

Figure 5. EF at A) smooth and B) rough gaps as a function of the gap distance *d* for symmetric gapped rods of 1200 nm segment length, irradiated with a 633 nm incident wavelength, with the electric component (E) and the wave vector (*k*) as depicted in the upper schemes.

cases, which correspond to the first maximum shown in Figure 3A, while the gap distance was varied every 4 nm. For smooth gap rods, when the segment length is fixed at values corresponding to maximum intensities (in this case 1200 nm), the maximum EF is obtained at a gap separation of 24 nm and a local maximum is observed at 12 nm (Figure 5A). For the rough gap rod (Figure 5B), the maximum is much broader and occurs at 56 nm, which is shifted towards bigger gap distances than for smooth gap rods. For rough segments, this shift occurs because a prominent tip in one segment may be closer to another tip in the opposite segment, thus reducing the effective gap distance.

In earlier work it was noted that the gaps generated by the OWL technique are rough and not perfectly perpendicular to the long axis of the rod.[13] Indeed, as can be seen from the SEM images (Figure 4 and Figure S2 in the Supporting Information), the gaps are neither sharp nor parallel at the edges. Previously, for 120 nm thick segments, it was shown that gap roughness significantly shifts the position of optimum gap size, from 12 nm for smooth particles to 32 nm for rough particles,[23,24] which is in agreement with the measured dependence of Raman intensity on gap size.[10] Thus, roughening reduces the sensitivity to precise structural features such that the theoretical and experimental results in Figure 3A are in very good agreement, even though we are comparing smooth rod results from theory with rough rod results from experiments. Indeed, the primary difference between theoretical (smooth rods) and experimental (rough rods) results lies in the absolute Raman intensities. This difference means that although the scaled intensities in Figure 3A agree, the scale factors are likely to be considerably different.

Another consequence of roughness arises in the dependence of the results on polarization. Several research groups have reported the dependence of SERS signal on the orientation of the particle's long axis relative to the polarization direction. Maximum enhancement is obtained when the laser is polarized along the long axis of the anisotropic particle,[25] that is, perpendicular to the gap.[26] These reports agree that the dependence of SERS intensity on the polarization angle is not as important for gap distances bigger than 10 nm. Since the gap sizes of the gapped structures we used were bigger than 15 nm, no intensity dependence was observed concerning the orientation of long axis of the rod with respect to the polarization of the incident light (data not shown).

In conclusion, it has been theoretically and experimentally demonstrated that the SERS intensity obtained at the gap of a long segment gapped Au structure has a periodic dependence on the length of the Au segment. The periodic dependence is determined by the SPP wavelength. There is also strong dependence on the gap size if the gap is smooth, but roughness significantly reduces this sensitivity, and it also quenches any effect of the polarization direction. The experimental results obtained herein along with the theoretical data, have allowed us to provide a conceptual understanding of the physical phenomena involved in Raman scattering from small nanogaps in long segment Au structures. In addition, the results point to a way of optimizing gap size and segment length such that one can create structures that are large enough to be addressed electrically but have a SERS enhancement that is sufficient to provide useful spectroscopic data. In particular, the results obtained here will be useful for constructing optimized devices that allow simultaneous electrical and SERS measurements of molecules immobilized within the nanogaps for application in molecular electronics[3] and analytical detection.[4]

Experimental Section

All chemicals and reagents were purchased from commercial sources and used as received. Methylene blue hydrate and 200 proof HPLC/spectrophotometric grade ethanol were purchased from Sigma–Aldrich, methanol from VWR, and H_2O_2 and ammonium hydroxide from Mallinckrodt Chemicals. Electroplating solutions were purchased from Technic Inc.

Gapped Au nanorods where created by OWL as previously described[1] using a 0.02 μm nominal pore diameter aluminum oxide membranes (Anodisc 47, 0.02 μm, Whatman–Schleicher&Schuell). For metal electroplating, a BAS 100 W potentiostat was used, in connection with a Pt wire as counterelectrode and a commercial Ag/AgCl reference electrode (BAS; see the Supporting Information for electroplating conditions).

Scanning electron microscopy (LEO 1525) was used for morphology measurements, and images were processed with GIMP 2 software for dimension analysis.

Rods were modified by immersion in a 1 mM ethanolic solution of methylene blue (MB) overnight. The rods were rinsed by localization at the bottom of the reaction vessel by centrifugation at 4600 rpm. The supernatant was discarded and the rods were resuspended in ethanol by sonication (3 s). This process was repeated 5 times.

Raman spectra (see the Supporting Information) were recorded with a confocal Raman microscope (WiTec Alpha 300) equipped with a piezo scanner and 100× microscope objective (n.a. = 0.90; Nikon,

Tokyo, Japan). Samples were excited with a 632.8 nm HeNe laser (Coherent, Inc., Santa Clara, CA) with a power density of approximately 10^4 W cm^{-2}, with the long axes of the nanowires parallel to the laser polarization.

All DDA calculations were carried out by DDSCAT7 with increments of 40 nm for the segment lengths and 4 nm for the gap distance variation.[27] The dielectric constant of Au was reported by Johnson and Christy.[28] The enhancement factors were calculated on a plane that is 2 nm away from the gap. Description of the rough surface construction for DDA calculations is described in the Supporting Information.

Received: August 20, 2009
Published online: December 3, 2009

Keywords: gold · nanostructures · on-wire lithography · surface-enhanced Raman scattering · surface plasmon resonance

[1] L. D. Qin, S. Park, L. Huang, C. A. Mirkin, *Science* **2005**, *309*, 113.
[2] W. Wei, S. Li, L. D. Qin, C. Xue, J. E. Millstone, X. Y. Xu, G. C. Schatz, C. A. Mirkin, *Nano. Lett.* **2008**, *8*, 3446.
[3] X. Chen, Y. M. Jeon, J. W. Jang, L. Qin, F. Huo, W. Wei, C. A. Mirkin, *J. Am. Chem. Soc.* **2008**, *130*, 8166.
[4] G. F. Zheng, L. D. Qin, C. A. Mirkin, *Angew. Chem.* **2008**, *120*, 1964; *Angew. Chem. Int. Ed.* **2008**, *47*, 1938.
[5] L. Qin, M. J. Banholzer, X. Xu, L. Huang, C. A. Mirkin, *J. Am. Chem. Soc.* **2007**, *129*, 14870.
[6] B. K. Oh, S. Park, J. E. Millstone, S. W. Lee, K. B. Lee, C. A. Mirkin, *J. Am. Chem. Soc.* **2006**, *128*, 11825.
[7] S. J. Hurst, E. K. Payne, L. D. Qin, C. A. Mirkin, *Angew. Chem.* **2006**, *118*, 2738; *Angew. Chem. Int. Ed.* **2006**, *45*, 2672.
[8] L. Qin, M. J. Banholzer, J. E. Millstone, C. A. Mirkin, *Nano. Lett.* **2007**, *7*, 3849.
[9] W. Wei, S. Li, J. E. Millstone, M. J. Banholzer, X. Chen, X. Y. Xu, G. C. Schatz, C. A. Mirkin, *Angew. Chem.* **2009**, *121*, 4274; *Angew. Chem. Int. Ed.* **2009**, *48*, 4210.
[10] L. D. Qin, S. L. Zou, C. Xue, A. Atkinson, G. C. Schatz, C. A. Mirkin, *Proc. Natl. Acad. Sci. USA* **2006**, *103*, 13300.
[11] X. Chen, A. B. Braunschweig, M. J. Wiester, S. Yeganeh, M. A. Ratner, C. A. Mirkin, *Angew. Chem.* **2009**, *121*, 5280; *Angew. Chem. Int. Ed.* **2009**, *48*, 5178.
[12] B. He, T. J. Morrow, C. D. Keating, *Curr. Opin. Chem. Biol.* **2008**, *12*, 522.
[13] S. Link, M. A. El-Sayed, *J. Phys. Chem. B* **1999**, *103*, 8410.
[14] E. R. Encina, E. A. Coronado, *J. Phys. Chem. C* **2007**, *111*, 16796.
[15] E. K. Payne, K. L. Shuford, S. Park, G. C. Schatz, C. A. Mirkin, *J. Phys. Chem. B* **2006**, *110*, 2150.
[16] E. S. Barnard, J. S. White, A. Chandran, M. L. Brongersma, *Opt. Express* **2008**, *16*, 16529.
[17] J. Dorfmuller, R. Vogelgesang, R. T. Weitz, C. Rockstuhl, C. Etrich, T. Pertsch, F. Lederer, K. Kern, *Nano. Lett.* **2009**, *9*, 2372.
[18] C. J. Murphy, A. M. Gole, S. E. Hunyadi, J. W. Stone, P. N. Sisco, A. Alkilany, B. E. Kinard, P. Hankins, *Chem. Commun.* **2008**, 544.
[19] Y. C. Cao, *J. Am. Chem. Soc.* **2004**, *126*, 7456.
[20] P. K. Jain, M. A. El-Sayed, *J. Phys. Chem. C* **2008**, *112*, 4954.
[21] A. M. Funston, C. Novo, T. J. Davis, P. Mulvaney, *Nano Lett.* **2009**, *9*, 1651.
[22] C. A. Pfeiffer, E. N. Economou, K. L. Ngai, *Phys. Rev. B* **1974**, *10*, 3038.
[23] M. J. Banholzer, S. Z. Li, J. B. Ketter, D. I. Rozkiewicz, G. C. Schatz, C. A. Mirkin, *J. Phys. Chem. C* **2008**, *112*, 15729.
[24] S. Li, G. C. Schatz, *Mater. Res. Soc. Symp. Proc.* **2008**, *1087*, 1087V0108.
[25] Y. Sawai, B. Takimoto, H. Nabika, K. Ajito, K. Murakoshi, *J. Am. Chem. Soc.* **2007**, *129*, 1658.
[26] J. M. Baik, S. J. Lee, M. Moskovits, *Nano. Lett.* **2009**, *9*, 672.
[27] B. T. Draine, P. J. Flatau, **2008**, http://arxiv.org/abs/0809.0337.
[28] P. B. Johnson, R. W. Christy, *Phys. Rev. B* **1972**, *6*, 4370.

